Chemical Physics Letters 507 (2011) 69–73

Contents lists available at ScienceDirect

Chemical Physics Letters

journal homepage: www.elsevier.com/locate/cplett

Femtosecond photolysis of CH_2Br_2 in acetonitrile: Capturing the bromomethyl radical and bromine-atom charge transfer complex through deep-to-near UV probing

Suman K. Pal [1], Andrey S. Mereshchenko, Patrick Z. El-Khoury [2], Alexander N. Tarnovsky *

Department of Chemistry and Center for Photochemical Sciences, Bowling Green State University, Bowling Green, OH, USA

ARTICLE INFO

Article history:
Received 13 December 2010
In final form 22 February 2011
Available online 4 March 2011

ABSTRACT

Dibromomethane (CH_2Br_2) in acetonitrile is a suitable precursor to characterize the absorption signatures of the $CH_2Br^{\cdot}$ radical and solvent $^{\cdot}Br$ charge-transfer complexes. Following irradiation of CH_2Br_2 at 255 nm, the *iso*-H_2C—Br—Br isomer product rapidly converts back to the parent species, and transient absorption spectra reveal the bands of solvent-separated radical species, the $CH_2Br^{\cdot}$ radical peaking at 235 nm, as well as the $CH_3CN{\cdot}Br$ complex at 272 nm. The absorption of $CH_2Br^{\cdot}$ exhibits minor solvatochromic shifts upon going from acetonitrile to cyclohexane, and the molecular decadic extinction coefficient of $CH_3CN{\cdot}Br$ is estimated to be 1470 M^{-1} cm^{-1}.

1. Introduction

Halogen atoms and halomethyl radicals are important intermediates in a large number of gas- and solution-phase photochemical reactions [1–9]. Capturing the electronic spectra of these species is critical to elucidate their role in atmospheric and environmental chemistry [8,10–19]. The electronic structure of these species is the basis for their absorption in the deep-UV/UV spectral regions, frequently masked by the overlapping absorption of other involved intermediates and photoproducts. In solvents, these radicals are even more elusive by nature, e.g. because of facile reaction with the solvent [10,12,17,18,20]. Therefore, finding suitable precursors for halomethyl radicals which allow capturing their transient spectral signatures in solution is a real challenge. An ideal precursor is one that dissociates in a predictable fashion to yield the radical of interest, with by-products absorbing at different wavelengths. If other photoproducts or intermediates form, they should ideally decay to recover the parent molecule relatively fast to unveil the spectral signatures of the radical species of interest.

We recently reported on the ultrafast UV photochemistry of CH_2Br_2 in acetonitrile by means of femtosecond transient absorption spectroscopy [21]. Irradiation of CH_2Br_2 using 255 nm laser pulses results in the formation of an isomer product, *iso*-H_2C—Br—Br. This isomer forms with a time constant of 8.5 ps and exhibits a broad, weak absorption band in the visible region (338–612 nm). The *iso*-H_2C—Br—Br product quickly decays back to the parent molecule with a 96-ps time constant, the absorption of *iso*-H_2C—Br—Br completely vanishing within ~250 ps after the pump pulse. Transient absorption (ΔA) spectra in the visible range and a selected deep-UV ΔA kinetics trace measured at 220 nm suggested that solvent separation of the $CH_2Br^{\cdot}$+$Br^{\cdot}$ radical pair competes with the formation of the *iso*-H_2C—Br—Br product [21]. These observations render CH_2Br_2 as a good precursor for the characterization of the $CH_2Br^{\cdot}$ and $Br^{\cdot}$ radicals in solution.

In this Letter, we report, for the first time, the UV-absorption spectra of the $CH_2Br^{\cdot}$ radical in acetonitrile and cyclohexane. The vertical transition energies of $CH_2Br^{\cdot}$ in the gas phase and different solvent environments are calculated. The polarizable continuum model (PCM) of solvation and hybrid quantum mechanics/molecular mechanics (QM/MM) calculations predict small solvatochromic shifts for the $CH_2Br^{\cdot}$ absorption. Moreover, the absorption spectrum of a charge-transfer complex (CTC) between a $Br^{\cdot}$ atom and acetonitrile is reported. The absorption bands of the CT complexes between $Br^{\cdot}$ and other solvents have been previously reported, but to the best of our knowledge, not in acetonitrile. We estimate an extinction coefficient of the $CH_3CN{\cdot}Br$ CT complex absorption to be ~1470 M^{-1} cm^{-1}. Additional experiments in which $Br^{\cdot}$ is scavenged by bromide (Br^-) support this finding.

2. Experimental and computational methods

The ultrafast transient absorption set-up used in this work has been previously described [21,22]. Briefly, a regeneratively amplified Ti:sapphire laser system (Hurricane, Spectra-Physics) generates a 1 kHz train of 90-fs (fwhm), 800-nm laser pulses with an energy of 0.92 mJ $pulse^{-1}$. The amplified output is 50:50 split into

* Corresponding author.
E-mail address: atarnov@bgsu.edu (A.N. Tarnovsky).
[1] Present address: School of Basic Sciences, Indian Institute of Technology (IIT), Mandi, Himachal Pradesh 175 001, India.
[2] Present address: Department of Chemistry, University of California, Irvine, California 92697-2025, USA.

0009-2614/$ - see front matter © 2011 Elsevier B.V. All rights reserved.
doi:10.1016/j.cplett.2011.02.046

two beams. The first beam is delivered to a TOPAS-C 'pump' optical parametric amplifier (Light Conversion Ltd.) to generate the second harmonic of the sum frequency of the signal output (SHSFS), 255-nm pulses of energy 4–6 μJ used for sample excitation. The second beam is delivered to a TOPAS-C 'probe' optical parametric amplifier to produce deep-UV/near-UV probe pulses. The beam was further split 40:10 with the largest portion delivered to the TOPAS-C to generate: (i) the fourth harmonic of the signal output, FHS probe pulses tunable from 275 to 400 nm, (ii) sum-frequency of the FHS output and 10% portion of the amplified beam, probe pulses tunable from 210 to 265 nm, (iii) the second harmonic of the sum frequency of the signal and fundamental outputs, SHSFS probe pulses tunable from 233 to 265 nm. The CH_2Br_2 (60 mM) and C_6H_5Br (25 and 50 mM) solutions are flown either through a jet of 0.3 mm pathlength or circulated through a Spectrosil quartz flow cell of 0.2 mm pathlength. All ΔA data were collected under magic angle (54.7°) polarization conditions and corrected for group velocity dispersion of the probe pulses. Transient absorption experiments are performed at room temperature using commercially available CH_2Br_2 (purity > 99%, Aldrich), C_6H_5Br (purity > 99%, Aldrich), tetrabutylammonium bromide (purity > 99%, Fluka) and spectroscopic-grade solvents. Tetrabutylammonium bromide was used as a source of bromide ions. The decomposition of samples during the experiments was negligible, as evidenced by UV/Vis spectra acquired before and after the measurements.

Unconstrained geometry optimization was performed using the UB3LYP and UM062X density functionals to locate the minima on the ground state potential energy surface (PES). All stationary points were characterized by calculating the associated vibrational frequencies. The aug-cc-pVXZ-PP series (X = D, T, and Q) which constitute a logical sequence of basis sets that converges towards the basis set limit were tested. We found that: (i) the geometrical parameters are almost converged with respect to a further increase in basis set description (from a triple ζ to a quadruple ζ description, and (ii) unlike the TD B3LYP vertical excitation energies, the TD M06-2x values converge towards the experimental value with a systematic increase in the basis set description. To simulate solvent effects on the calculated vertical transition energies, the PCM solvation model was used to simulate both acetonitrile and cyclohexane. In addition, we predict the vertical transition energies of the $CH_2Br^{\cdot}$ radical in methanol using the ONIOM (DFT:UFF) method. The solvated system was separated into two parts treated at different levels of theory. The $CH_2Br^{\cdot}$ radical treated at the QM level (DFT/aug-cc-pVXZ) and the surrounding solvent molecules treated the MM level (UFF). A pre-equilibrated cubic methanol box of 10 Å centered at the solute was employed. The UFF force-field parameters were used for $CH_2Br^{\cdot}$, its RESP point charges generated at the HF/6-31G* level. Vertical transition energies were calculated at the TD-DFT/UFF//DFT/UFF level of theory. All calculations were performed using the methodologies implemented in GAUSSIAN 09 [23].

3. Results and discussion

Two experimental absorption spectra of $CH_2Br^{\cdot}$ in the gas phase were previously reported [14,19]. Villenave and Lesclaux [19] found a band peaking at 43 200 cm^{-1} (231 nm) using flash photolysis, in disagreement with a spectrum consisting of two bands at 35 520 cm^{-1} (281 nm) and 40 260 cm^{-1} (248 nm) measured by Nielsen et al. [14] using the $F^{\cdot}$+CH_3Br reaction in which the $F^{\cdot}$ radicals were generated by pulse radiolysis irradiation of SF_6 (Figure 1). Villenave and Lesclaux [19] argued that the data reported by Nielsen et al. [14] are contaminated by secondary chemistry. Subsequently, Nielsen and co-workers showed that their earlier spectrum contained contamination from a $CH_3Br^{\cdot}F$ charge-transfer complex [24]. Transient resonance Raman spectra of $CH_2Br^{\cdot}$ in solution were measured by Chong et al. [25] following excitation of CH_2Br_2 at 239.5 nm (cyclohexane), 239.5 and 228.7 nm (methanol), suggesting that this radical absorbs at these wavelengths. Their time-dependent random phase calculations predict that the only singlet transition of $CH_2Br^{\cdot}$ above 200 nm is centered at 255 nm (with an oscillator strength, f = 0.0011). MRCI/CASSF calculations of $CH_2Br^{\cdot}$ by Li et al. [26] predict the first excited state to be at 279 nm (f = 0.0001), the second symmetry-forbidden transition at 258 nm, and the third excited state at 221 nm of a significant intensity (f = 0.0500). At the MS-CASPT2 level, the first three electronic transitions of $CH_2Br^{\cdot}$ have low oscillator strengths, whereas the fourth transition at 230 nm is intense (f = 0.045) [27]. Thus, the MRCI and MS-CASPT2 calculations give support to a single absorption band of $CH_2Br^{\cdot}$ as measured by Villenave and Lesclaux [19], although the MRCI transition energies seem to be somewhat overestimated (Figure 1).

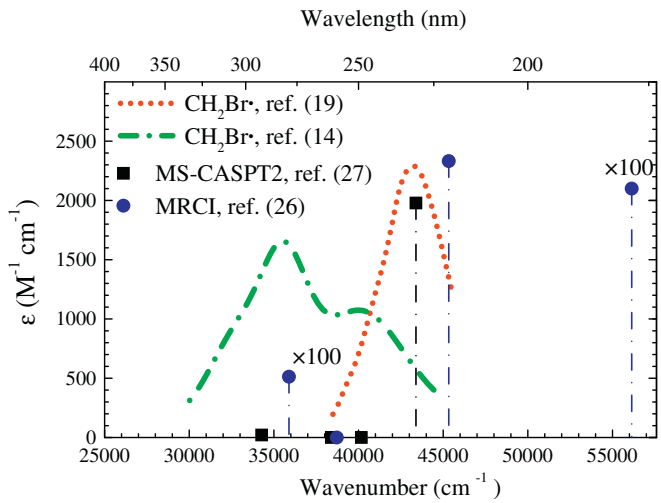

Figure 1. UV molar decadic extinction of the CH_2Br radical in gas phase, experiments: (solid line [19] and dotted line [14]), and calculations: (●) MRCI (26), (■) MS-CASPT2 [27]. The MS-MRCI and CASPT2 oscillator strengths from [26,27] were recalculated into molecular extinctions according to Eq. (18) of [27] to facilitate the comparison with the experimental spectra.

In this work, the absorption spectrum of $CH_2Br^{\cdot}$ was obtained by measuring transient absorption ΔA spectra of CH_2Br_2 in acetonitrile and cyclohexane in the deep-UV/UV range at relatively long delay times (500 and 1000 ps) between pump and probe pulses after the complete decay of the *iso*-H_2C—Br—Br isomer product. The measured ΔA spectra display two pronounced bands, an intense absorption between 210 and 250 nm with a maximum signal at 235 nm, and a weaker absorption between 250 and 320 nm peaking at 272 nm, Figure 2. The use of dilute (⩽60 mM) CH_2Br_2 solutions and the observation that the ΔA kinetic traces in the investigated spectral range do not depend on CH_2Br_2 concentration [21] indicates negligible contribution from CH_2Br_2·Br CT complex under the experimental conditions employed in this study. For CH_2Br_2 in cyclohexane, the deep-UV ΔA spectra also exhibit a band maximum at ~235 nm (Figure 3). No appreciable solvatochromic shifts were observed in the 235 nm band upon going from acetonitrile to cyclohexane (Figure 3).

As (i) the 235 nm band is observed in both solvents employed in this work, (ii) the 272 nm band only recorded in acetonitrile, and (iii) the absorption of the Br-cyclohexane CTC is known to peak at 370 nm [28], the 235 nm band can be tentatively assigned to $CH_2Br^{\cdot}$. This is supported by vertical transition energy calculations of $CH_2Br^{\cdot}$ in the gas phase as well as in solution environments (acetonitrile, cyclohexane and methanol) at the UB3LYP and UM062X

levels of theory. The vertical transition energies of five lowest excited states of $CH_2Br^{\cdot}$ in the gas phase are presented in Table 1 along with the previously reported values. Both the UB3LYP and UM062X methods predict that the most intense transition in the gas phase is the fourth. The calculated UM062X transition energies exhibit a convergence towards the experimental value with a systematic increase in basis set description (Table S1, Supporting information), where the UB3LYP transition energies unsystematically diverge from the experimental value with an increase of basis set description (Table S2, Supporting information). In our previous works, we employed M062X functional to describe a variety of systems, CF_2I_2, and CF_2Br_2 [29,30]. We recently tested the performance of the UM062X functional in describing the different possible structures of the $C_2H_4Br^{\cdot}$ radical [31]. Among the different density functionals and ab initio methods employed, the UM062X functional yielded the best agreement with the high level CCSD calculations for this open shell system. In the current work, the TD UMO62X results and CASPT2 vertical transition energies are found to be in very close agreement, suggesting that this density functional is also suitable for the calculation of structures and UV–Vis spectra of this halomethyl radical. Furthermore, the UB3LYP/aug-cc-pvQZ and UM062x/aug-cc-pvQZ transition energies of $CH_2Br^{\cdot}$ in various solvents are given in Table 2. Vertical transition energies are very similar in acetonitrile, cyclohexane, and methanol with negligible solvatochromic shifts (Table 2), as evidenced by TDDFT/PCM as well as TDDFT/UFF calculations.

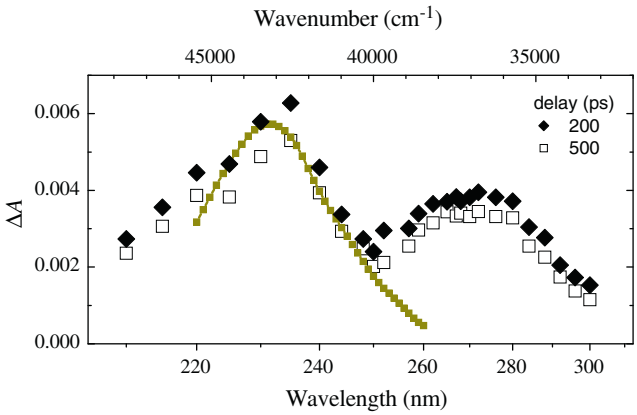

Figure 2. Transient absorption spectra (symbols) of a 60-mM CH_2Br_2 acetonitrile solution measured 200 and 500 ps after 255-nm excitation. With increasing time delay, two 235- and 272-nm product bands assigned to $CH_2Br^{\cdot}$ and $CH_3CN{\cdot}Br$ CTC decay uniformly, consistent with geminate recombination. The absorption spectrum of gas-phase $CH_2Br^{\cdot}$ reported in [19] is shown for comparison (symbols connected by lines).

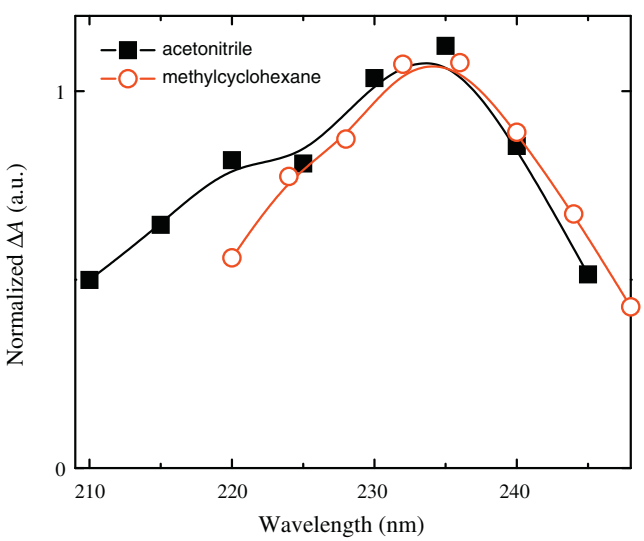

Figure 3. Normalized ΔA spectra of CH_2Br_2 in acetonitrile assigned to absorption of the $CH_2Br^{\cdot}$ radicals in acetonitrile (squares) and cyclohexane (circles).

The 272 nm band in acetonitrile is assigned to the $CH_3CN{\cdot}Br$ CT complex. According to Mulliken [32], the ground and excited states of a 1:1 CT complex can be described by a linear combination of the no-bond (ψ_0) and dative (ψ_1) wave-functions. The absorption maximum of a CT band, as a function of vertical ionization potential (I_D) of a solvent-donor molecule, is described by the following relation [33–36]:

$$E_{CT} = \frac{1}{1-S^2}\left[(I_D - C)^2 + 4\beta_0\beta_1\right]^{1/2} \quad (1)$$

where, S is the overlap integral, β_0 and β_1 are the resonance integrals related as follows: $\beta_1 = \beta_0 - S(I_D - C)$, and $C = E_A + G_1 - G_0$, E_A is the electron affinity of the acceptor and G_0 and G_1 are the dissociation energies of the complex in its pure no-bond and dative states, respectively. The correlation between the absorption maximum of a CT complex and the ionization potential of a donor according to Eq. (1) is known to be well obeyed by halogen atom-solvent complexes in both polar and non-polar solvents [13,33,37]. Treinin and Hayon [13] observed the absorption

Table 1
Vertical transition energies (nm) of the $CH_2Br^{\cdot}$ radical in the gas phase calculated using the aug-cc-pVQZ basis set. The corresponding oscillator strengths are given in parentheses.

UB3LYP	UM062X	CASSCF[a]	MRCI[a]	MS-CASPT2[b]
308.39 (0.0029)	305.30 (0.0020)	262.16	278.65 (0.0001)	291.76 (0.0005)
293.88 (0.0000)	272.45 (0.0000)	238.46	258.33 (0.0000)	260.50 (0.0000)
250.84 (0.0002)	242.17 (0.0004)	206.32	**220.64 (0.0500)**	248.99 (0.0000)
242.04 (0.0568)	**229.45 (0.0576)**	171.51	178.16 (0.0004)	**230.48 (0.0452)**
217.96 (0.0000)	214.04 (0.0000)	154.23	157.66 (0.0000)	–––––

[a] Ref. [26], oscillator strengths (f) were calculated using the relation $f = 2/3\,|\Delta m^2|\,E$, where Δm is the transition dipole moment change, E is the MRCI vertical transition energy.
[b] Ref. [27].

Table 2
Vertical transition energies (nm) of the $CH_2Br^{\cdot}$ radical in different solvents calculated using the aug-cc-pVQZ basis set. Corresponding oscillator strengths are given in parentheses.

Medium	UB3LYP	UM062X
Acetonitrile (PCM)	307.15 (0.0029)	305.74 (0.0019)
	287.39 (0.0000)	265.96 (0.0000)
	250.85 (0.0000)	241.22 (0.0002)
	239.38 (0.0695)	**225.10 (0.0711)**
	214.37 (0.0000)	210.19 (0.0000)
Cyclohexane (PCM)	308.23 (0.0031)	305.79 (0.0021)
	291.24 (0.0000)	269.75 (0.0000)
	251.16 (0.0001)	242.03 (0.0003)
	242.47 (0.0730)	**228.92 (0.0744)**
	216.50 (0.0000)	212.46 (0.0000)
Methanol (PCM)	307.14 (0.0028)	305.72 (0.0019)
	287.41 (0.0000)	265.98 (0.0000)
	250.83 (0.0000)	241.21 (0.0002)
	239.33 (0.0690)	**225.07 (0.0706)**
	214.38 (0.0000)	210.21 (0.0000)
Methanol (Oniom (QM/MM))	308.06 (0.0029)	302.04 (0.0023)
	293.85 (0.0000)	273.78 (0.0000)
	250.90 (0.0002)	240.24 (0.0004)
	241.91 (0.0570)	**230.36 (0.0569)**
	218.01 (0.0000)	212.35 (0.0000)

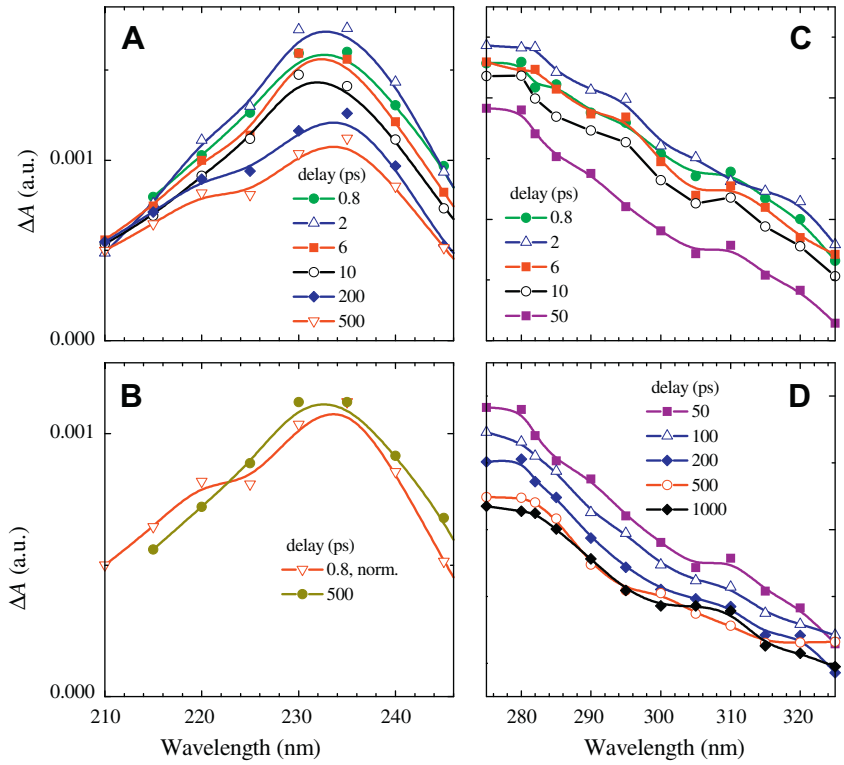

Figure 4. Measured transient absorption ΔA spectra of CH_2Br_2 (60 mM) in acetonitrile after 255-nm excitation. Panel A: the ΔA spectra assigned to absorption of $CH_2Br^{\cdot}$ radicals. Panel B: the normalized 0.8- and 500-ps ΔA spectra from Panel A. Panels C and D: the ΔA spectra measured in the absorption range of the $CH_3CN{\cdot}Br$ CT complexes at short and long delay times.

maximum of Br atoms and water CT complex at 275 nm. As the ionization potential of acetonitrile (12.2 eV) is less than water (12.6 eV), the band maximum of $CH_3CN{\cdot}Br$ CT complex is expected to lie at ~300 nm, consistent with the assignment of the 272 nm band. As for cyclohexane (I_D = 9.86 eV), a broad absorption peak of $C_6H_{10}{\cdot}Br$ was located at 370 nm following laser photolysis of Br_2 in this solvent [28].

Based on the relative amplitude of the 235- and 272-nm bands, and under the assumption that the maximum molecular decadic extinction coefficient of $CH_2Br^{\cdot}$ remains the same in the gas-phase and solution (ε = 2300 M^{-1} cm^{-1} [19]), the ε value of $CH_3CN{\cdot}Br$ CT complex is estimated to be ~1470 M^{-1} cm^{-1}. A straightforward correction of this value to the spectral overlap between the absorption spectra of $CH_2Br^{\cdot}$ and CH_2Br_2 (ε = 500 M^{-1} cm^{-1} at 240 nm), assuming equimolar amounts of the $CH_2Br^{\cdot}$ formation and ground-state depletion, yields an extinction of ε = 1200 M^{-1} cm^{-1}.

Bromobenzene (C_6H_5Br) has been used as precursor of $Br^{\cdot}$ atom in a number of time-resolved investigations on a tens of nanosecond time scale, Eq. (2), [13,38].

$$C_6H_5Br \xrightarrow{h\nu} C_6H_5^{\cdot} + Br^{\cdot} \tag{2}$$

The photolysis reaction, on a sub-1 ns time scale has been found to involve long-lived species attributed to lower-lying triplet states in C_6H_5Br [39].

Indeed, the long-time (500 ps) ΔA spectra of C_6H_5Br in acetonitrile following 255-nm excitation display intense transient absorption peaking in the deep-UV, displaying a shoulder at 280 nm, resembling the absorption band of $CH_3CN{\cdot}Br$ CTC. Measurement of the ΔA spectra of C_6H_5Br in acetonitrile in the presence of bromide ion (Br^-) gives further support to this assignment. In the presence of Br^- (0.5 M), the absorption band around 280 nm decays on a 250-ps time scale with a concomitant formation of a new absorption band at ~360 nm identical to that reported for Br_2^- [40,41]. The decay time of the 280-nm band and rise time of the 360 nm band of Br_2^- become longer with decreasing concentration of Br^-, consistent with scavenging of $Br^{\cdot}$ (or, $CH_3CN{\cdot}Br$ CTC) by Br^- via Eq. (3).

$$Br^{\bullet} + Br^- \Longleftrightarrow Br_2^{\bullet -} \tag{3}$$

Assuming that the 290-nm ΔA signal is entirely due to the $CH_3CN{\cdot}Br$ CTC, undergoing full conversion into Br_2^-, the ε value of $CH_3CN{\cdot}Br$ CTC is determined using Eq. (4):

$$\varepsilon(CH_3CN \cdot Br) = \varepsilon(Br_2^-)_{360} \frac{\Delta A(CH_3CN \cdot Br)}{\Delta A(Br_2^-)_{360}} \tag{4}$$

Here, the ΔA is the change in the transient absorption between 250 ps (ΔA signal levels off indicating that scavenging is complete) and the extrapolated 0 ps ΔA signal measured at 290 nm for ΔA(Br) (in the presence of Br^-) and 360 nm for $\Delta A(Br_2^-)$. From the known extinction of Br_2^- at 360 nm, $\varepsilon(Br_2^-)$ = 9900 M^{-1} cm^{-1} [42], the value of $\varepsilon(CH_3CN \cdot Br)$ at 290 nm is calculated to be ~890 M^{-1} cm^{-1}. Based on this value, GAUSSIAN deconvolution of the 235 and 272 nm bands due to $CH_2Br^{\cdot}$ and $CH_3CN{\cdot}Br$ CT (Figure 1S, Supporting information) results in a value of ε = 1364 M^{-1} cm^{-1} for $CH_3CN{\cdot}Br$ at the absorption maximum. So far, the following ε values were reported: 23 700 M^{-1} cm^{-1} (λ_{max} = 550 nm) for $C_6H_6{\cdot}Br$ (π-complex between bromine atom and arene [43]), 2800 ± 500 M^{-1} cm^{-1} (λ_{max} = 560 nm) for $C_6H_5Br{\cdot}Br$ [38], 3500 ± 500 M^{-1} cm^{-1} (λ_{max} = 275 nm) for $H_2O{\cdot}Br$, [13] and 4000 M^{-1} cm^{-1} for $C_6H_5{\cdot}Br$ [44].

Having established the spectral signatures of $CH_2Br^{\cdot}$ and $CH_3CN{\cdot}Br$ CT products, we now can inspect the short-time ΔA signal spectra of CH_2Br_2 to determine the onset of formation of these species (Figure 4). Short-time transient absorption up to 0.5 ps is mainly due to solvent signal. At 0.8 ps, the solvent signal decays, but the intense 235-nm feature is already formed. The transient absorption decays with a 9-ps time constant, leading to the isomer

formation. On a much slower time scale between 500 and 1000 ps, the 235-nm band somewhat decays. This attributed to secondary geminate recombination. In the spectral range corresponding to the $CH_3CN{\cdot}Br$ CT absorption, the 0.8-ps ΔA spectra undergo rise and decay to the 272-nm band at long times (500 ps). The observation that this evolution is accompanied by only a minor re-shaping of the ΔA spectra probably suggest that the $CH_3CN{\cdot}Br$ CT complex is already present at 0.8 ps. This is consistent with the previously observed time scale for the onset of formation of CT complexes involving halogen atoms [16,45].

4. Conclusions

The absorption band of the $CH_2Br^{\cdot}$ radical species and the Br atom CT complex with acetonitrile are reported in this work for the first time, assigned on the basis of TD DFT calculations and carefully designed scavenging experiments. Recording the spectral signatures of the cage-escaped radical species is made possible as a result of the fast decay (~250 ps) of the primary geminate recombination product, the *iso*-H_2C—Br—Br species. These results open ways to future studies requiring clearly defined spectral signatures of these species, for example, the two *vs* three body decay mechanisms in CH_2Br_2 and structurally related halogenated alkanes in solution.

Acknowledgements

This work was supported by the NSF CAREER award (Grant CHE-0847707, ANT). An allocation of computer time from the Ohio Supercomputer Center is gratefully acknowledged.

Appendix A. Supplementary data

Supplementary data associated with this article can be found, in the online version, at doi:10.1016/j.cplett.2011.02.046.

References

[1] L.A. Barrie, J.W. Bottenheim, R.C. Schnell, P.J. Crutzen, R.A. Rasmussen, Nature 334 (1988) 138.
[2] L.J. Carpenter, Chem. Rev. 103 (2003) 4953.
[3] H. Sato, Chem. Rev. 101 (2001) 2687.
[4] W.R. Simpson et al., Atmos. Chem. Phys. 7 (2007) 4375.
[5] V.A. Apkarian, N. Schwentner, Chem. Rev. 99 (1999) 1481.
[6] P.J. Reid, Acc. Chem. Res. 34 (2001) 691.
[7] M.A. Miranda, J. Pérez-Prieto, E. Font-Sanchis, J.C. Scaiano, Acc. Chem. Res. 34 (2001) 717.
[8] C.G. Elles, Rev. Phys. Chem. 57 (2006) 273.
[9] C.D. O'Dowd et al., Nature 417 (2002) 632.
[10] L.C.T. Shoute, P. Neta, J. Phys. Chem. 94 (1990) 7181.
[11] C. Maul, C. Dietrich, T. Haas, K.-H. Gericke, Phys. Chem. Chem. Phys. 1 (1999) 1441.
[12] F. Wicktor, A. Donati, H. Herrmann, R. Zellner, Phys. Chem. Chem. Phys. 5 (2003) 2562.
[13] A. Treinin, E. Hayon, J. Am. Chem. Soc. 97 (1975) 1716.
[14] O.J. Nielsen, J. Munk, G. Locke, T.J. Wallington, J. Phys. Chem. 95 (1991) 8714.
[15] P.Z. El-Khoury, L. George, A. Kalume, I. Schapiro, M. Olivucci, A.N. Tarnovsky, S.A. Reid, Chem. Phys. Lett. 496 (2010) 68.
[16] C.G. Elles, M.J. Cox, G.L. Barnes, F.F. Crim, J. Phys. Chem. A 108 (2004) 10973.
[17] L. Sheps, A.C. Crowther, C.G. Elles, F.F. Crim, J. Phys. Chem. A 109 (2005) 4296.
[18] L. Sheps, A.C. Crowther, S.L. Carrier, F.F. Crim, J. Phys. Chem. A 110 (2006) 3087.
[19] E. Villenave, R. Lesclaux, Chem. Phys. Lett. 236 (1995) 376.
[20] D. Raftery, M. Iannone, C.M. Phillips, R.M. Hochstrasser, Chem. Phys. Lett. 201 (1993) 513.
[21] P.Z. El-Khoury, S.K. Pal, A.S. Mereshchenko, A.N. Tarnovsky, Chem. Phys. Lett. 493 (2010) 61.
[22] P.Z. El-Khoury, A.N. Tarnovsky, Chem. Phys. Lett. 453 (2008) 160.
[23] M.J. Frisch et al., GAUSSIAN 09, Gaussian Inc., Wallingford, CT, 2009.
[24] J. Sehested, M. Bilde, T. Mogelberg, T.J. Wallington, O.J. Nielsen, J. Phys. Chem. 100 (1996) 10989.
[25] C.K. Chong, X.M. Zheng, D.L. Phillips, Chem. Phys. Lett. 328 (2000) 113.
[26] Y.M. Li, J.S. Francisco, J. Chem. Phys. 114 (2001) 2879.
[27] T. Rozgonyi, L. Gonzalez, J. Phys. Chem. A 106 (2002) 11150.
[28] Z.B. Alfassi, R.E. Huie, J.P. Mittal, P. Neta, L.C.T. Shoute, J. Phys. Chem. 97 (1993) 9120.
[29] P.Z. El-Khoury, L. George, A. Kalume, S.A. Reid, B.S. Ault, A.N. Tarnovsky, J. Chem. Phys. 132 (2010) 124501.
[30] L. George, A. Kalume, P.Z. El-Khoury, A.N. Tarnovsky, S.A. Reid, J. Chem. Phys. 132 (2010) 084503.
[31] A. Kalume, L. George, P.Z. El-Khoury, A.N. Tarnovsky, S.A. Reid, J. Phys. Chem. A 114 (2010) 9919.
[32] R.S. Mulliken, J. Am. Chem. Soc. 74 (1952) 811.
[33] R.E. Buhler, J. Phys. Chem. 76 (1972) 3220.
[34] G. Briegleb, Elektronen-Donator-Akzeptor Komplexe, Springer-Verlag, West Berlin, 1961.
[35] W.B. Person, R.S. Mulliken, Molecular Complexes: A Lecture and Reprint Volume, Wiley, New York, NY, 1970.
[36] R.S. Mulliken, W.B. Person, Ann. Rev. Phys. Chem. 13 (1962) 107.
[37] R.E. Buhler, Radiat. Res. Rev. 4 (1972) 233.
[38] J.M. Bossy, R.E. Btthler, M. Ebert, J. Am. Chem. Soc. 92 (1970) 1099.
[39] M. Rasmusson et al., Chem. Phys. Lett. 367 (2003) 759.
[40] L.I. Grossweiner, M.S. Matheson, J. Phys. Chem. 81 (1957) 1089.
[41] D. Zehavi, J. Rabani, J. Phys. Chem. 76 (1972) 312.
[42] G.L. Hug, Optical Spectra of Nonmetallic Inorganic Transient Species in Aqueous Solution, US Department of Commerce, National Bureau of Standards, Washington, DC, 1981.
[43] W.G. McGimpsey, J.C. Scaiano, Can. J. Chem. 66 (1988) 1474.
[44] P. Fornier de Violet, Rev. Chem. Interm. 4 (1981) 121.
[45] N. Pugliano, A.Z. Szarka, S. Gnanakaran, M. Triechel, R.M. Hochstrasser, J. Chem. Phys. 103 (1995) 6498.